Journal of Oleo Science
Copyright ©2019 by Japan Oil Chemists' Society
doi : 10.5650/jos.ess18127
J. Oleo Sci. **68**, *(8) 699-707 (2019)*

Effect of Oil Content on Physiochemical Characteristics of γ-Oryzanol-Loaded Nanostructured Lipid Carriers

Warangkana Pornputtapitak[1]*, Jaturavit Pantakitcharoenkul[1], Veerawat Teeranachaideekul[2], Kitiphat Sinthiptharakoon[3], Chaweewan Sapcharoenkun[3], and Benchaporn Meemuk[3]

[1] *Department of Chemical Engineering, Faculty of Engineering, Mahidol University, Nakhon Pathom 73170, THAILAND*
[2] *Department of Pharmacy, Faculty of Pharmacy, Mahidol University, Bangkok 10400, Thailand*
[3] *National Nanotechnology Center (NANOTEC), National Science and Technology Development Agency (NSTDA), Pathum Thani 12120, THAILAND*

Abstract: Nanostructured lipid carriers (NLCs) are used as alternative carriers for many different drug delivery administration routes. They are composed of both solid lipid and liquid lipid (oil content) with both influencing their structural properties. Amounts of liquid lipid in NLCs play a role in drug release. Effect of liquid lipid (oil content) on physiochemical characteristics of NLCs related to drug-release requires detailed investigation. Here, many techniques were performed to analyze the physiochemical characteristics of NLCs, especially inside the particles. γ-Oryzanol (GO)-loaded NLCs were prepared at varying solid lipid to liquid lipid ratios. Their physicochemical properties, drug release profiles, and stability studies of prepared NLCs were investigated. Oil contents in NLCs were found to play a significant role in physiochemical characteristics related to drug release and stability, and also influence the efficiency of analytical techniques such as transmission electron microscopy (TEM) and dynamic force microscopy (DFM). Moreover, x-ray diffraction (XRD) and Fourier transform infrared spectroscopy (FTIR) gave information regarding crystallinity inside the NLCs. FTIR showed broad peaks in the range from 1184 cm^{-1} to 1475 cm^{-1} while XRD presented a broad curve indicated amorphous forms in NLCs. Orthorhombic lattices (β' polymorph) were also elucidated by XRD and differential scanning calorimetry (DSC).

Key words: nanostructured lipid carriers, γ-oryzanol, analytical techniques, physiochemical characteristic

1 Introduction

Lipid nanoparticles are used as an alternative to traditional carriers such as nanoemulsion, liposomes and polymeric nanoparticles for different routes of pulmonary[1)], oral[2)] and dermal[3)] administration. Their advantages include biocompatibility, possibility of large-scale production, organic solvent free synthesis and controlled drug release[4, 5)]. Over the last two decades, lipid nanoparticles have developed from first generation of solid lipid nanoparticles (SLNs) to second generation of nanostructured lipid carriers (NLCs) by adding liquid lipid into particles instead of using only solid lipid. Liquid lipid interrupts polymorphic transformation that is the main cause of drug expulsion during storage of SLNs. Therefore, oil contents in NLCs play a role in the polymorphic forms of lipid matrix and their performance.

γ-Oryzanol (GO) is a natural component found in rice bran and rice germ. It consists of at least 10 components[6)], but five major components are cycloartenyl ferulate, 24-methylene cycloartanyl ferulate, campesteryl ferulate, the combination of β-sitosteryl ferulate and cycloartanyl ferulate, and sitostanyl ferulate[7)]. GO is an antioxidant compound, which is excellent in inhibiting lipid peroxidation and reducing cholesterol oxidation[8)]. It is a promising ingredient for cosmetic applications. It occurs at up to 10 times higher than vitamin E in rice bran with significantly higher antioxidant activity[7, 9)]. Moreover, GO acts as a UV-A filter that could be used in sunscreen cosmetics[10)]. Recently, GO was found in Leum Pua glutinous rice bran. The release profile of γ-oryzanol extract was slightly higher

*Correspondence to: Warangkana Pornputtapitak, Department of Chemical Engineering, Faculty of Engineering, Mahidol University, Nakhon Pathom 73170, THAILAND
E-mail: warangkana.por@mahidol.edu
Accepted April 17, 2019 (received for review July 3, 2018)
Journal of Oleo Science ISSN 1345-8957 print / ISSN 1347-3352 online
http://www.jstage.jst.go.jp/browse/jos/ http://mc.manusriptcentral.com/jjocs

than standard γ-oryzanol, although initial amounts of γ-oryzanol were similar[7], due to different oil contents in the extracts. Study of how oil content influences drug release, stability and physiochemical characteristics is important regarding development of cosmetic products.

In this study, NLCs were prepared using high pressure homogenization (HPH). GO was loaded in NLCs at various liquid lipid to solid lipid ratios up to 50%. Characteristics of NLCs were investigated by dynamic light scattering (DLS) to compare particle size distribution and morphology using transmission electron microscopy (TEM) and atomic force microscopy (AFM) with tapping mode. Crystallinity of NLCs was determined using X-ray diffraction (XRD) and Fourier transform infrared spectroscopy (FTIR) and compared with differential scanning calorimetry (DSC). Comparisons between important pieces of information from each technique were noted and discussed.

2 Experimental

2.1 Materials

Cetyl palmitate and caprylic/capric triglycerides were purchased from Namsiang Group (Bangkok, Thailand). γ-Oryzanol, Tween80 (Polysorbate 80) and Span40 (Sorbitan monopalmitate) were purchased from Sigma-Aldrich (Japan). Methanol, acetonitrile, and isopropanol were purchased from RCI Labscan (Bangkok, Thailand). Distilled water and deionized water were prepared freshly from Autostil™ 8000x (England) and aquaMax™-Ultra (Korea), respectively. Phosphate buffer saline (PBS) pH 5.5 was prepared freshly in the laboratory. All other chemicals were commercially available in analytical grade and used without further purification.

2.2 Preparation of nanostructured lipid carriers (NLCs)

Nanostructured lipid carriers (NLCs) were prepared by hot high-pressure homogenization (HPH). Lipid phase containing cetyl palmitate as a solid lipid, caprylic/capric triglycerides as a liquid lipid and Span 40 as a lipophilic surfactant were melted together at 80℃. The aqueous phase containing Tween 80 as a hydrophilic surfactant was heated to 80℃ and then added to the lipid phase. The mixture was homogenized at 8,000 rpm for 1 min using a homogenizer (ULTRA-TURRAX® T25, IKA). The pre-emulsion was continuously heated until temperature reached 80℃ and then processed by a high-pressure homogenizer (High Pressure Homogenizer® APV-2000) for 3 cycles at 500 bar. Obtained NLCs were cooled down under ambient conditions to room temperature and 0.2 wt% of DMDM hydantoin was added as a preservative. Nanoemulsion (NE) and GO-loaded NLC formulations were prepared in the same manner. For NE formulation, only liquid lipid was used, whereas for GO-loaded NLC formulations, 1 wt% GO was added to the lipid phase before pre-emulsion preparation step. NLC formulations were composed of 10 wt.% total lipid contents and 4 wt.% surfactants. Tween 80 and Span 40 were used as co-surfactants at a 1:1 ratio in all experiments. Solid lipid to liquid lipid ratios of NLCs was studied at 50:50 (NLC55), 70:30 (NLC73) and 90:10 (NLC91).

2.3 Particle size measurement

Particle size analysis was performed by Malvern Zetasizer Nano-ZS (Malvern Instruments, UK) at a scattering angle of 173° using folded capillary cell (DTS1060). Samples were prepared by 10 fold dilution with deionized water. Mean particle size and polydispersity index (PI) were obtained by the average of five measurements and all experiments were done in triplicate.

2.4 The morphology determination

Morphology of NLC was observed by TEM (TECNAI T20 G^2, FEI Company, USA) and AFM (SPA400, Hitachi High-Tech, Japan) using AFM with tapping mode as dynamic force microscopy (DFM). For TEM determination, samples were prepared by spreading the sample on a 300-mesh copper grid before coating with 2% uranyl acetate (BDH Chemicals Ltd, England) for negative staining. Prepared samples were dried under ambient conditions overnight before TEM investigation. For AFM determination utilized silicon tips (HA_HR, NT-MDT, Russia) with tip curvature radius of less than 10 nm, resonant frequency of approximately 230 kHz, and 17 N/m force constant. Tapping-mode AFM, alternatively called dynamic force microscopy (DFM)[11, 12], in which the tip oscillated over the sample with transient contact with the sample surface at the oscillation bottom, was used. Each formulation of appropriate amount was diluted with deionized water and subsequently deposited on a clean glass substrate. Samples were then air-dried overnight prior to imaging. All images were obtained under ambient conditions with a slow scan speed of around 0.5 Hz and high oscillating amplitude to avoid the tip dragging on the sample.

2.5 Differential scanning calorimetry (DSC)

Degree of crystallinity of NLC formulations was performed using a differential scanning calorimeter (DSC Q200 TA Instruments). Samples were placed in a 40 μL aluminum pan with an empty pan used as a reference. Samples were exposed to two cycles of heat and cool by scanning from 0℃ to 85℃ at heating rate of 5℃/min and then cooling to 0℃ at the same rate. Melting onset temperature, melting point temperature, and melting enthalpy were determined. Crystallinity index (%CI) was calculated using equation 1[13].

$$\% \text{ CI} = \frac{\Delta H_{NLC\ aqueous\ dispersion\ (J/g)}}{\Delta H_{bulk\ material\ (J/g)} \times Concentration_{lipid\ phase\ (\%)}} \times 100 \quad (1)$$

2.6 X-ray diffraction (XRD) analysis

Polymorphic forms of prepared NLCs were investigated using XRD on PANalytical X'Pert PRO (PANalytical, the Netherlands) with a copper anode (Cu Ka radiation, 45 kV, 45 mA, k = 0.154056 nm) at room temperature. NLC dispersions were transformed into a paste by mixing with locust bean gum powder. Samples were scanned from 3 to 40 with a step width of 0.02 (0.5 s/ step) and d-spacing values were calculated by the Bragg's equation.

2.7 Fourier transform infrared (FTIR) spectroscopy

Before FTIR determination, NLC samples were lyophilized for 24 hours to eliminate water. Then, dry NLC samples were blended with KBr and pressed into pallets. Infrared spectra of NLC formulations were scanned on a JASCO FTIR-6800 spectrometer (Tokyo, Japan), at 4 cm^{-1} resolution with frequency range between 400 and 4000 cm^{-1}.

2.8 Reverse phase high pressure liquid chromatography (RP-HPLC)

RP-HPLC was performed by using Waters Alliance 2695 HPLC Separations module (Waters Corporation, Milford, USA), equipped with aWaters® 2489 UV/Visible detector. Samples were separated using a Sunfire C18 column with 4.6 × 100 mm diameter (3.5 μm) at a flow rate of 0.8 mL/ min and 20 μl injection volume. Total run time for each sample was 20 min at a wavelength of 325 nm[7]. A mixture of acetonitrile, methanol and isopropanol (45:30:25% (v/v)) was used as the mobile phase. Standard GO was prepared in drug release medium (phosphate buffer saline (PBS), pH 5.5, 50% isopropanol and 5% tween80).

2.9 Drug encapsulation efficiency (%EE)

Encapsulation efficiency (%EE) was indirectly determined by centrifugal filtration using a centrifugal filter tube (Amicon® Ultra-15, 30 kDa molecular weight cut-off, Millipore, Ireland). Four grams of sample were placed into a centrifugal filter tube and centrifuged at 5000 g for 30 min at room temperature. The supernatant was collected and examined for amount of GO by RP-HPLC. Percentage of EE (%EE) was calculated by equation 2.

$$\% \text{ EE} = \frac{Total\ amount\ of\ drug\ put\ in\ formulation - Amount\ of\ unloaded\ drug\ in\ NLC}{Total\ amount\ of\ drug\ put\ in\ formulation} \times 100 \quad (2)$$

2.10 *In vitro* release study

Static vertical Franz diffusion cells were used to determine the amount of GO released from the prepared formulations. GO was diffused through mixed cellulose ester membrane filters with pore size diameter of 0.1 μm (Advantec®, Japan). Surface area of 2.0 cm^2 was used as release membrane with acceptor medium as a mixture of phosphate buffer saline (PBS, pH 5.5), isopropanol and Tween 80 at ratio of 50:50:5. The medium was stirred using a magnetic bar to avoid concentration differences and minimize stagnant layers. Temperature was controlled at 32℃ to mimic human skin. Then, 300 μL of NLC formulation were loaded onto the membrane in the donor compartment with 0.5 mL of receptor medium collected at 2, 4, 6, 8, 10, 12 and 24 hours using a syringe needle and replaced with the same volume of freshly prepared receptor medium. Collected samples were analyzed by the RP-HPLC method as described previously. Sink conditions were maintained over the experiments. The experiments were performed in triplicate. Data were presented as mean values ± standard deviation (SD).

2.11 Statistical analysis

Data for particle size measurements were presented as mean values ± standard deviation (SD). Statistical significance of difference was examined using one-way ANOVA at probability level of 0.05. The Tukey HSD (Honestly Significant Difference) post-hoc test was applied to indicate significant differences between the groups at 95% confidence intervals.

3 Results and Discussion

3.1 Particle size Analysis

NLC particle size gradually reduced with increasing liquid lipid content up to 50% (**Table 1**). Mean particle size of NLCs decreased from 151.7 ± 1.6 nm to 144.3 ± 2.3 nm and 129.3 ± 2.0 nm when increasing liquid lipid contents from 10% to 30% and 50%, respectively ($p < 0.05$). High liquid lipid content decreased viscosity inside NLCs, resulting in small particles due to low surface tension. However, size of nanoemulsion (NE) containing 100% liquid lipid and 0% solid lipid didnot differ from NLCs with 50% oil content. Moreover, the optimal ratio also depended on types of liquid lipid. Hu *et al.*[14] found unchanged sizes of NLCs if oleic acid (liquid lipid) was less than 15 wt% but significant reduced sizes of NLCs if oleic acid was more than 30 wt%.

Polydispersity index (PI) of all formulations was around 0.1 with a monodisperse pattern size distribution plot indicating excellent quality of particle dispersion. In general, PI ranges from 0 to 1. The lower the PI, the better the quality of particle size distribution in suspension with 0.5 PI as acceptable[15]. However, PI value lower than 0.3 have also been suggested as optimal[16].

Table 1 Mean particle size and polydispersity index (PI) of GO-loaded NLC and NE formulations stored at 4℃ and room temperature for 12 weeks.

Formulation	Week 0		Particle size (nm)			
	Particle size (nm)	Polydispersity index (PI)	4℃		Room temperature	
			Week 6	Week 12	Week 6	Week 12
GO-loaded NLC55	129.3 ± 2.0	0.105 ± 0.015	135.2 ± 0.6	140.0 ± 0.6	126.7 ± 0.4	124.2 ± 2.3
GO-loaded NLC73	144.3 ± 2.3	0.102 ± 0.037	156.8 ± 5.1	155.0 ± 1.3	142.3 ± 2.8	137.8 ± 1.5
GO-loaded NLC91	151.7 ± 1.6	0.119 ± 0.013	150.2 ± 1.7	152.2 ± 1.1	154.4 ± 1.3	155.9 ± 3.5
GO-loaded NE	132.8 ± 0.3	0.055 ± 0.035	133.3 ± 4.2	130.1 ± 2.2	129.1 ± 0.4	132.8 ± 1.2

3.2 Stability study

NLC formulations were stored at 4℃ and at room temperature for 12 weeks to examine stability. Mean particle size of GO-loaded NLCs did not change with temperature. PI values of all NLC formulations ranged around 0.1-0.2 throughout the storing period indicating good quality of particle dispersion. This result was inconsistent with previously reported significant changes in particle size when NLCs and SLNs were stored at 25℃[17], possibly explained by differing qualities of NLC particles. According to the mean particles size of around 430 nm reported in literature, possibility of aggregation increased when NLCs were stored for long time periods[17]. Here, NLC formulations had mean particle sizes lower than 200 nm, with results showing excellent physical stability over 12 weeks. Thus, it could be hypothesized that aggregation rarely occurred for particle sizes around 200 nm or lower. This assumption was supported by results confirming no change in NLC particles of around 200 nm stored at room temperature for 3 months[18]. For larger NLC particles, storage at a lower temperature might improve physical stability through reduction of kinetic energy in the system. However, although mean particle size of NE was as small as GO-loaded NLC55 and did not significantly change over 12 weeks (Table 1), the PI of NE increased slightly faster when stored at room temperature compared to 4℃.

Zeta potentials of NLC formulations were around −20 mV to −30 mV. Zeta potential indicates probable physical stability of the colloidal dispersion and can be positive or negative. Absolute value presents the degree of repulsion between particles in the formulation, resulting in prevention of particle aggregation during storage. Most NLC or SLN formulations have a negative value of zeta potential. Stable SLN formulations have a zeta potential lower than −25 mV, whereas samples with zeta potential of −15 mV or higher tend to show gelation phenomena[5]. Here, all formulations were stable during storage since zeta potential was lower than −15 mV. This result was confirmed by mean particle size measured by DLS during storage (Table 1). Moreover, non-ionic surfactants can help to prevent agglomeration of NLCs due to steric stabilization[15]. For NE formulation, zeta potential changed from −24.8 ± 0.7 mV to −28.5 ± 1.4 mV and −34.0 ± 0.7 mV when kept at 4℃, whereas it changed to −24.4 ± 0.1 mV and −16.9 ± 0.4 mV when kept at room temperature. Therefore, NE formulation should be stored at low temperature for long-term storage to decrease kinetic energy of the particles.

3.3 Particle morphology characterization

Morphology of NLC particles was investigated by TEM and AFM with tapping mode called dynamic force microscope (DFM).

3.3.1 TEM investigation

NLC formulations were prepared by negative staining coating before recording TEM images. Quality of prepared particles was not the same for three TEM images, displaying particles in the range 120-180 nm, and prepared following exactly the same procedure (Fig. 1). This might be due to different physical properties of the particles caused by disparate amounts of liquid lipid.

Spherical and anisometric shaped particles were found in GO-loaded NLC55 whereas more spherical particles were shown by the others. The TEM image of GO-loaded NLC55 also displayed some smaller particles around 10-30 nm (Fig. 1a). These smaller particles were not detected by DLS which can measure particle size down to 0.3 nm but did not register these few tiny particles compared to the larger majority. These smaller particles should be taken into account to better comprehend NLC production.

3.3.2 AFM investigation

Particle size and morphology of NLC formulations were also performed by AFM with the tapping mode (DFM). Topography images and phase images were investigated for each sample. However, due to a bury characteristic of NLC nanoparticles in the samples prepared using the formulated materials, it was nearly impossible to observe the nanocarriers. Particle feature could be seen using phase images related to elasticity of the particles in the same imaging area (Fig. 2). Based on these images, size of observed particles mostly ranged between 100 nm and 150 nm, consistent with the DLS results. Any size deviation from this range was attributed to the bury characteristic of the nanoparticles. Phase images showed that NLC nanoparticles were spherical in shape, especially for GO-loaded

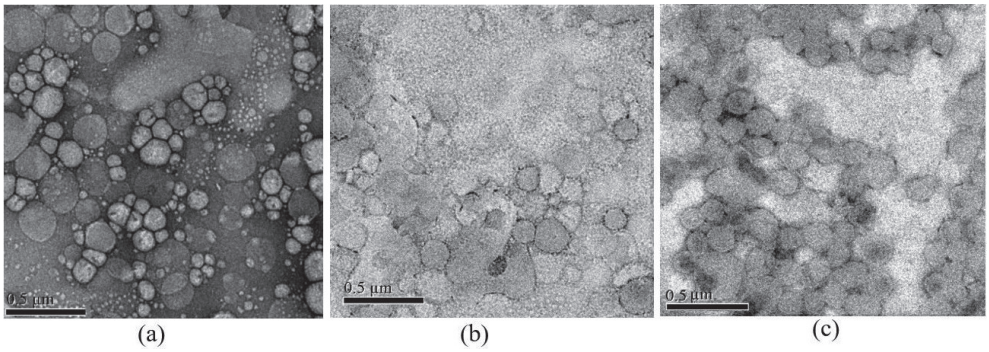

Fig. 1 TEM images of NLC particles: (a)γ-oryzanol-loaded NLCs with solid lipid to liquid lipid ratio of 50:50(GO-loaded NLC55), (b)70:30(GO-loaded NLC73), and(c)90:10(GO-loaded NLC91).

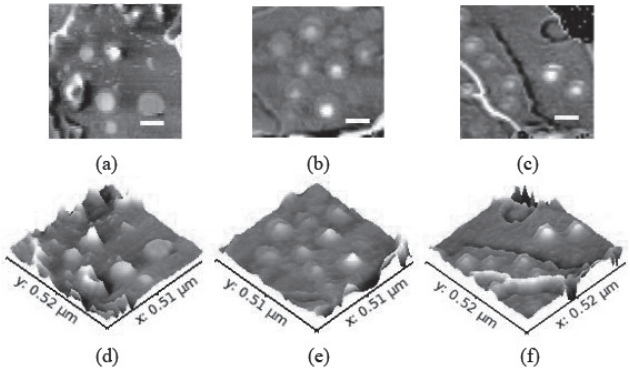

Fig. 2 DFM phase images of NLC particles at solid lipid to liquid lipid ratios of(a)50:50, (b)70:30, (c)90:10 along with their related 3D views(d)-(f). Each white scale bar is 100 nm long.

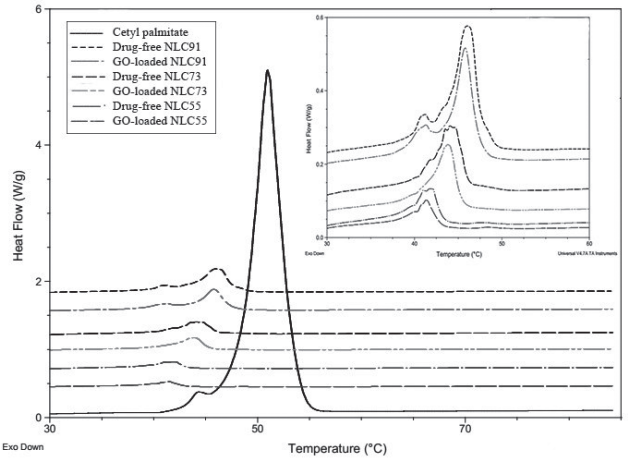

Fig. 3 DSC thermogram of drug-free NLC and GO-loaded NLC formulations with different solid lipid to liquid lipid ratios.

NLC73 and GO-loaded NLC91, whereas some anisometrically shaped particles were also found for GO-loaded NLC55, consistent with TEM images. As mentioned previously, DFM as a tapping-mode AFM maintained less contact of the tip and the sample through intermittent contact between the sample surface and the vibrating cantilever instead of tracing the tip across the sample. Consequently, the sample was less damaged by drag force pulling sideways. However, contact was still slightly affected due to softer particles of GO-loaded NLC55 compared to other formulations. This also made it more difficult to obtain a good image for GO-loaded NLC55.

3.4 Differential scanning calorimetry(DSC)investigation

DSC was performed to investigate the degree of crystallinity(%CI)and identify the polymorphism of prepared NLCs. Bulk cetyl palmitate had a main endothermic peak at 50.93℃, and a smaller endothermic peak at around 44℃ (Fig. 3). In general, a triacylglycerol possesses three polymorphic forms as an amorphous α-form, metastable β'-form, and stable β-form[19]. The α-form is less dense than other forms and tends to change to a more stable form to reduce the Gibbs free energy of the system. The β'-form is an intermediate packing, usually presented since transformation from α-form to β'-form is faster than crystallization of stable β-form without passage through β'-form. Therefore, the densest packing of stable β-form, which has lower Gibbs free energy, will melt at the highest temperature on the DSC thermogram followed by β'-form and α-form, respectively. The β'-form normally appears as a shoulder of the main melting peak[20]. However, in some cases such as mixed-acid triacylglycerol, no β-form was found and β'-form became the most stable form in the system[19]. The polymorphic form of all formulations was further confirmed by XRD analysis.

Melting onset and melting peak temperature of NLC formulations were shifted toward lower temperature. Melting enthalpy decreased due to small particle size with high surface area, and presence of surfactants[21]. Lipid matrices of NLCs should be a less ordered polymorph compared to bulk cetyl palmitate for which melting enthalpy was set at 100% crystallinity as a reference. The%CI of NLC decreased, especially when increasing oil contents in the formulation(Table 2).

Table 2 DSC parameters of NLC formulations.

Formulation	Melting onset (℃)	Melting peak temperature (℃)	Enthalpy change (J/g)	CI (%)
Cetyl palmitate	48.59	50.93	226.70	100
Drug-free NLC55	39.47	41.68	4.16	37
Drug-free NLC73	42.21	44.01	7.86	50
Drug-free NLC91	43.81	46.00	15.61	77
GO-loaded NLC55	39.67	41.31	3.05	27
GO-loaded NLC73	41.30	43.81	7.11	45
GO-loaded NLC91	43.70	45.81	13.70	67

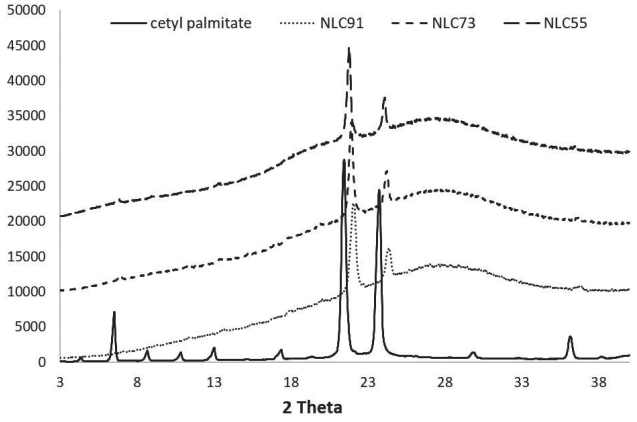

Fig. 4 X-ray diffraction (XRD) patterns of γ-oryzanol-loaded NLCs with varying solid lipid to liquid lipid ratios of cetyl palmitate.

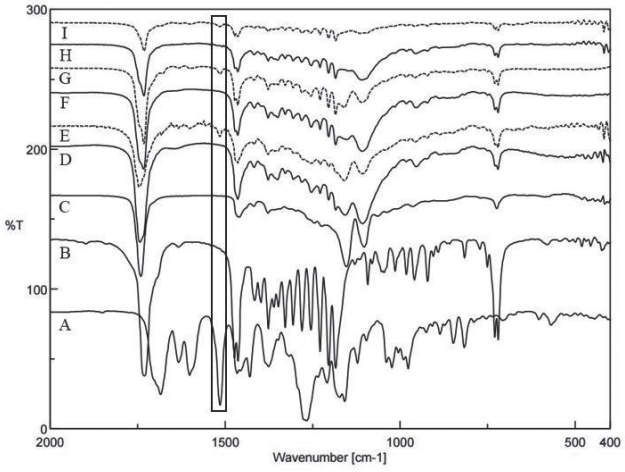

Fig. 5 FTIR spectra of (A) γ-oryzanol (GO), (B) cetyl palmitate, (C) caprylic/capric triglycerides, (D) drug-free NLC55, (E) GO-loaded NLC55, (F) drug-free NLC73, (G) GO-loaded NLC73, (H) drug-free NLC91, and (I) GO-loaded NLC91. The rectangular box indicates peak GO detected on GO-loaded NLC formulations.

Normally, the endothermic melting peak of GO occurs at around 60-80℃; however, on peak was found on the DSC thermogram of GO-loaded NLC formulations, possibly because GO dissolved in the lipid matrix. The %CI of NLCs decreased slightly when GO loading increased, although no significant difference was shown between DSC thermograms of GO-loaded and drug-free NLCs. Consequently, melting enthalpy of GO-loaded NLCs could not be seen on the DSC thermogram. However, the existence of GO was confirmed by FTIR.

3.5 X-ray diffraction (XRD) analysis

X-ray diffraction (XRD) analysis was performed to investigate the polymorphic behavior and crystallinity of cetyl palmitate after NLC production. XRD patterns of bulk cetyl palmitate (Fig. 4) indicated orthorhombic lattices (β' polymorph) with a lattice spacing of 0.38 and 0.42 nm[22, 23]. Diffraction pattern of bulk cetyl palmitate showed shape peaks with no maxima, indicating a highly crystalline form. NLC formulations with varying oil contents showed peaks at similar position; however, a broad curve also appeared which was attributed to amorphous form. Thus, lipid matrices of NLCs included β'-polymorph and amorphous form. This result concurred with DSC investigations that showed less crystallinity of lipid matrices with increasing oil content.

3.6 Fourier transform infrared (FTIR) investigation

Fourier transform infrared (FTIR) spectroscopy is used to detect conformation of lipid molecules in matrices by demonstrating functional groups in chemical structures and determining chemical interactions among molecules in mixtures. Here, FTIR spectra of NLCs were compared to those of γ-oryzanol (A), cetyl palmitate (B), and caprylic/capric triglycerides (C) to investigate chemical interactions between the compounds (Fig. 5). The FTIR spectra of NLC formulations showed main peaks at the same wavenumber as combinations of individual compounds. Shifting of peaks or invoking new peaks were not found. This indicated no chemical interaction among lipid and drug molecules. Therefore, only physical interaction was suggested for this system[24]. The FTIR spectrum of cetyl palmitate in the

range of 1184 cm^{-1} to 1475 cm^{-1} gave many sharp peaks due to bending vibration of CH_3, CH_2 and CH bonds in the range of 1350-1470 cm^{-1} and stretching vibration of the single C-O bond at 1210-1320 cm^{-1}. Sharp peaks in this range had some benefits on the elucidation of crystallinity in NLC particles[25]. For cetyl palmitate, broad peaks were found in a similar range, indicating a less ordered structure in the lipid matrix. Moreover, crystallinity of lipid matrices was related to the amount of liquid lipid in the formulation. For GO-loaded NLC formulations, the higher the liquid lipid content, the higher the amorphous state of lipid matrices. The FTIR spectrum of GO-loaded NLC55 showed broad peaks. Some disappeared at 1184 cm^{-1} to 1475 cm^{-1} because the formulation contained 50 wt% of liquid lipid. Similarly, the FTIR spectrum of caprylic/capric triglycerides (C) did not show any sharp peaks in this range since caprylic/capric triglycerides were measured in liquid form with no crystallinity in the sample. Differences in FTIR spectra between drug-free NLC formulations and GO-loaded NLC formulations were also examined. Spectra of GO-loaded NLCs showed a peak at 1515 cm^{-1} due to C=C in arenes of GO. This confirmed the existence of GO in NLC formulations (Fig. 5).

3.7 Encapsulation efficiency

Encapsulation efficiency (%EE) was high in all NLC formulations. This can be explained by the lipophilicity of GO that prefers lipid phase to aqueous phase. Encapsulation efficiency of the lipophilic drug increased when the liquid lipid in NLCs increased. In general, NLCs with a higher percentage of liquid lipid gave higher percent drug loading and percent drug entrapment[17]. However, although drug loaded in NLCs tended to be better dissolved in liquid lipid than solid lipid, the %EE of these NLC formulations was not significantly different ($p>0.05$) because GO was almost insoluble in water. The %EE of GO-loaded NLC55, GO-loaded NLC73, GO-loaded NLC91 and GO-loaded NE were 99.939 ± 0.019, 99.936 ± 0.019, 99.935 ± 0.018 and 99.945 ± 0.018, respectively.

3.8 *In vitro* release studies

Release profiles of NLC and NE formulations showed that higher percentage of liquid lipid provided higher drug release (Fig. 6). The release profile of GO-loaded NE was observed as a linear line followed Fick's law of diffusion. GO-loaded NLC55 showed a release profile close to NE formulation. Generally, release profiles of drug from lipid nanoparticles such as SLNs or NLCs have two states. The initial state shows fast release since drug content dissolved in the outer shell of particles is released easier than drug content inside the particles. The second state involves prolonged release of the drug inside the particles. A release profile was proposed to follow Stokes-Einstein equation because lipid matrices have high viscosity which slows

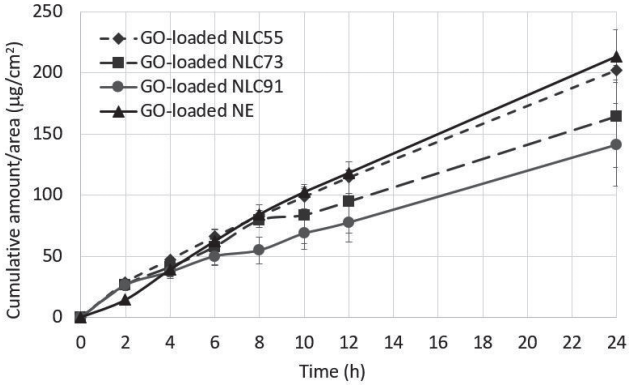

Fig. 6 Cumulative amount per unit area (μg/cm^2) of γ-oryzanol (GO) released from NLCs and NE formulations over 24 hours.

down the release profile[13], especially for SLNs containing only solid lipid in the lipid matrix. If burst release was excluded, the best fit for SLN release profile followed the Higuchi model[26] which states that drug release from particles is proportional to the square root of time[27]. However, in this study, release of GO from NLC particles did not followed the Higuchi model for initial state (<8 hours) but could be described by the Higuchi model after 8 hours release time (data not shown). Burst release was not found at the initial state of time profiles since the %EE of all formulations was 99.9%. However, when considering the cumulative release profile of NLC formulations, the release was still faster at the initial state, especially for the first two hours. In the first two hours, no difference of drug release was found among NLC formulations. Thus, initial release was attributed to the drug on the outer shell or surface of NLC particles. After 2 hours, the amount of liquid lipid in the NLC formulations became a factor that affected the rate of GO release. The higher amount of liquid lipid gave faster release. As discussed previously, lipid matrices made from solid lipid slowed down drug release. This effect was minimized when increasing liquid lipid content in the lipid matrices. Since liquid lipid was less viscous than solid lipid, the influence of solid lipid matrices was decreased. According to the DSC thermograms and XRD patterns, less ordered polymorphs and amorphous forms were found, especially for GO-loaded NLC55. This allowed the drug to pass through lipid matrices easier than the rigid ones.

4 Conclusion

Oil contents had an influence on drug release performance. Higher oil contents in NLCs gave faster release. However, no significant difference of release profile was found between NLCs with 100% and 50% oil contents. Moreover, burst release was not found for all formulations

since %EE of all GO-loaded NLC was 99.9%. Oil contents not only affected release performance but also directly related to information obtained from each technique as well as image quality from TEM and AFM. Consequently, intensive preparation is required for higher liquid lipid component samples. Moreover, FTIR was determined as an interesting technique for further study regarding other applications besides identifying functional group. Amorphous forms in NLCs were confirmed by broad peaks in the range 1184 cm^{-1} to 1475 cm^{-1} by FTIR, consistant with information from XRD patterns and DSC thermograms.

Acknowledgments

This work was financially supported by the National Research Council of Thailand (NRCT) and Agricultural Research Development Agency (Public Organization) under research grants (CRP5805020590). TEM observations were thanks to Thassanant Atithep, Center of Nanoimaging, Faculty of Science, Mahidol University. The authors are grateful to Faculty of Engineering and Faculty of Pharmacy, Mahidol University, and the National Nanotechnology Center (NANOTEC) for facility support.

Conflict of Interest

The authors declare no conflicts of interest.

REFERENCES

1) Weber, S.; Zimmer, A.; Pardeike, J. Solid lipid nanoparticles (SLN) and nanostructured lipid carriers (NLC) for pulmonary application: A review of the state of the art. *Eur. J. Pharm. Biopharm.* **86**, 7-22 (2014).
2) Das, S.; Chaudhury, A. Recent advances in lipid nanoparticle formulations with solid matrix for oral drug delivery. *AAPS PharmSciTech.* **12**, 62-76 (2011).
3) Müller, R.H.; Petersen, R.D.; Hommoss, A.; Pardeike, J. Nanostructured lipid carriers (NLC) in cosmetic dermal products. *Adv. Drug Deliv. Rev.* **59**, 522-530 (2007).
4) Zur Mühlen, A.; Schwarz, C.; Mehnert, W. Solid lipid nanoparticles (SLN) for controlled drug delivery – Drug release and release mechanism. *Eur. J. Pharm. Biopharm.* **45**, 149-155 (1998).
5) Mehnert, W.; Mäder, K. Solid lipid nanoparticles: Production, characterization and applications. *Adv. Drug Deliv. Rev.* **47**, 165-196 (2001).
6) Xu, Z.; Godber, J.S. Purification and identification of components of γ-oryzanol in rice bran oil. *J. Agric. Food Chem.* **47**, 2724-2728 (1999).
7) Pornputtapitak, W.; Pantakitcharoenkul, J.; Panpakdee, R.; Teeranachaideekul, V.; Sinchaipanid, N. Development of γ-oryzanol rich extract from Leum Pua glutinous rice bran loaded nanostructured lipid carriers for topical delivery. *J. Oleo Sci.* **67**, 125-133 (2018).
8) Hiramitsu, T.; Armstrong, D. Preventive effect of antioxidants on lipid peroxidation in the retina. *Ophthalmic Res.* **23**, 196-203 (1991).
9) Xu, Z.; Hua, N.; Godber, J.S. Antioxidant activity of tocopherols, tocotrienols, and γ-oryzanol components from rice bran against cholesterol oxidation accelerated by 2,2'-azobis (2-methylpropionamidine) dihydrochloride. *J. Agric. Food Chem.* **49**, 2077-2081 (2001).
10) Coppini, D.; Paganizzi, P.; Santi, P.; Ghirardini, A. Capacità protettiva nei confronti delle radiazioni solari di derivati di origine vegetale. *Cosmetic News* **136**, 15-20 (2001).
11) Garcia, R.; Gómez, C.J.; Martinez, N.F.; Patil, S.; Dietz, C.; Magerle, R. Identification of nanoscale dissipation processes by dynamic atomic force microscopy. *Phys. Rev. Lett.* **97**, 016103 (2006).
12) Giessibl, F.J. Forces and frequency shifts in atomic-resolution dynamic-force microscopy. *Phys. Rev. B* **56**, 16010-16015 (1997).
13) Teeranachaideekul, V.; Souto, E.B.; Junyaprasert, V.B.; Müller, R.H. Cetyl palmitate-based NLC for topical delivery of Coenzyme Q 10–Development, physicochemical characterization and *in vitro* release studies. *Eur. J. Pharm. Biopharm.* **67**, 141-148 (2007).
14) Hu, F.-Q.; Jiang, S.-P.; Du, Y.-Z.; Yuan, H.; Ye, Y.-Q.; Zeng, S. Preparation and characterization of stearic acid nanostructured lipid carriers by solvent diffusion method in an aqueous system. *Colloids Surf. B* **45**, 167-173 (2005).
15) Shah, R.; Eldridge, D.; Palombo, E.; Harding, I. Optimisation and stability assessment of solid lipid nanoparticles using particle size and zeta potential. *Journal of Physical Science* **25**, 59 (2014).
16) Kaur, I.P.; Bhandari, R.; Bhandari, S.; Kakkar, V. Potential of solid lipid nanoparticles in brain targeting. *J. Control. Release* **127**, 97-109 (2008).
17) Hu, F.-Q.; Jiang, S.-P.; Du, Y.-Z.; Yuan, H.; Ye, Y.-Q.; Zeng, S. Preparation and characteristics of monostearin nanostructured lipid carriers. *Int. J. Pharm.* **314**, 83-89 (2006).
18) Loo, C.H.; Basri, M.; Ismail, R.; Lau, H.L.N.; Tejo, B.A.; Kanthimathi, M.; Hassan, H.; Choo, Y.M. Effect of compositions in nanostructured lipid carriers (NLC) on skin hydration and occlusion. *Int. J. Nanomedicine* **8**, 13-22 (2013).
19) Sato, K. Crystallization behaviour of fats and lipids—a review. *Chem. Eng. Sci.* **56**, 2255-2265 (2001).
20) Bunjes, H.; Westesen, K.; Koch, M.H. Crystallization tendency and polymorphic transitions in triglyceride nanoparticles. *Int. J. Pharm.* **129**, 159-173 (1996).

21) Jenning, V.; Thünemann, A.F.; Gohla, S.H. Characterisation of a novel solid lipid nanoparticle carrier system based on binary mixtures of liquid and solid lipids. *Int. J. Pharm.* **199**, 167-177 (2000).
22) Jenning, V.;Gohla, S. Comparison of wax and glyceride solid lipid nanoparticles (SLN®). *Int. J. Pharm.* **196**, 219-222 (2000).
23) Lukowski, G.; Kasbohm, J.; Pflegel, P.; Illing, A.; Wulff, H. Crystallographic investigation of cetylpalmitate solid lipid nanoparticles. *Int. J. Pharm.* **196**, 201-205 (2000).
24) Pezeshki, A.; Ghanbarzadeh, B.; Mohammadi, M.; Fathollahi, I.; Hamishehkar, H. Encapsulation of vitamin A palmitate in nanostructured lipid carrier (NLC)-effect of surfactant concentration on the formulation properties. *Adv. Pharm. Bull.* **4**, 563 (2014).
25) Lin, X.; Li, X.; Zheng, L.; Yu, L.; Zhang, Q.; Liu, W. Preparation and characterization of monocaprate nanostructured lipid carriers. *Colloids Surf. A* **311**, 106-111 (2007).
26) Dash, S.; Murthy, P.N.; Nath, L.; Chowdhury, P. Kinetic modeling on drug release from controlled drug delivery systems. *Acta Pol. Pharm.* **67**, 217-223 (2010).
27) Ruktanonchai, U.; Sakulkhu, U.; Bejrapha, P.; Opanasopit, P.; Bunyapraphatsara, N.; Junyaprasert, V.; Puttipipatkhachorn, S. Effect of lipid types on physicochemical characteristics, stability and antioxidant activity of gamma-oryzanol-loaded lipid nanoparticles. *J. Microencapsul.* **26**, 614-626 (2009).